

NICMOS Coronagraphic Calibration

A.B. Schultz, G. Schneider, I. Dashevsky, D. Fraquelli, A. Welty, and E. Roye
February 4, 2004

ABSTRACT

The NICMOS coronagraphic imaging mode has been fully reactivated following SM3B, performing slightly better than during Cycle 7. The diffractive rejection is essentially unchanged (to first order) from Cycle 7 except there is a shift in the mean position of the cold mask which gives better second-order rejection on the downsloping diffraction spikes and slightly worse on the upsloping diffraction spikes. A target can be positioned within ~ 0.08 pixel (~ 5.8 mas) of the coronagraphic hole low-scatter position, with a repeatability of ~ 0.04 pixel (~ 2.9 mas) for two visits executed within the same orbit, with a roll between visits. The coronagraphic focus was checked and no adjustment was needed. The Cycle 7 coronagraphic focus position is still the best focus. A slight adjustment was made to the PAMC tilt to remove some coma that was not present during Cycle 7. The “hole 32x32 pixel subarray” field-of-regard (FOR) was adjusted by a few pixels in each direction due to displacement of the hole image on the detector caused by the warm up at the end of Cycle 7 and subsequent cool down following SM3B. A new ACQ FOR “gain” table (flat field) was installed to handle hot and cold pixels, allowing Mode-2 acquisitions for targets from $H=4$ to 17. The coronagraphic hole low scatter point, the “sweet spot,” was checked and a slight adjustment was required to achieve light suppression about the coronagraphic hole comparable to or slightly better than that achieved during Cycle 7.

Introduction

The Near Infrared Camera and Multi-Object Spectrometer (NICMOS) Camera 2 coronagraphic observing mode capability is provided by a small hole in the optical relay mirror on the Field-Divider Assembly (FDA) outside the dewar combined with a cold mask at the

entrance to the dewar. The hole (165 microns in diameter, giving a radius of $\sim 0.3''$) was created by boring through the back side of the optical relay mirror to within 1 mm of the mirror surface. The remaining glass was laser-ablated off the mirror. The image of the hole on the detector is offset from the center into one quadrant and near the edge of the detector.

Target Acquisition

NICMOS coronagraphy is extremely sensitive to small centering errors which can result from imperfections in the target acquisition (TA) process. During HST Cycle 7 the onboard TA process was augmented not only to locate the target, but also to determine the location of the hole in the ACQ image. This resulted in post-acquisition dispersions of target placements with respect to the fiducial position of 0.08 mas (or $\sim 1/10$ pixel). This level of acquisition precision is required so that high-contrast imaging near occulted targets may be achieved (Schultz et al. 1998, NICMOS-ISR-98-012).

Target acquisition is essentially a four step process; locate and centroid the target, locate and centroid the coronagraphic hole image, determine an offset between the target and hole position, and slew the telescope to move the image of the hole over the image of the target. These steps are performed by the Mode-2 acquisition onboard flight software (FSW) and a similar process can be performed on the ground for bright targets (for stars with $H < 4.0$ under the F187N filter) (Schultz et al. 1998, NICMOS-ISR-97-031).

Target Location

The FSW obtains two ACQ images using the exposure time specified in the Phase II file. The target is located in the Field-of-Regard (FOR) which is defined by a 128x128 pixel subarray. The position of the lower left-hand corner of the FOR is (66,35) in FSW detector coordinates. The "background" pixels in the FOR images all have values of about -210. This is due to the detector reset gradient (shading) in the image. The FSW image analysis algorithms need positive values to work correctly so a constant value of +500 is added to each pixel of the FOR images and then the two images are combined by minimization to remove cosmic ray (cr) strikes. The FSW then flat fields this image by multiplying it by an onboard "gain table" (inverse flat field reference data). Because the values in the gain table are integer, the multiplier values are scaled from 0 to 255, with the array median response at 100. The FSW actually divides the product of the multiplication by 255 to obtain flat fielded counts.

The "target location" algorithm used by the FSW "finds" the target by locating the 3x3 pixel subarray with the highest number of counts in the processed image. The target is then centroided using a 3x3 pixel checkbox. The FSW target location is saved and stored in the engineering snapshot attached to the next observation following the target acquisition (TA). The OPUS pipeline extracts this information and populates the Target Acquisition Keywords in the science header. The location is given in detector coordinates.

The IMAGE coordinate systems for NICMOS cameras have been defined such that the origin will be in the lower left hand corner when displayed using IRAF, while detector coordinates (DEC) are defined by the readout directions for each camera. Any NICMOS image when displayed using the IRAF **display** command will be displayed relative to the HST Field-of-View (FOV) as depicted in the NICMOS Instrument Handbook. The position and plate scale information for each NICMOS aperture is kept in the Science Instrument Aperture File (SIAF) in the HST Project Reference Database (PRD a.k.a PDB).

Hole Location

The onboard “hole-finding” process involves locating the hole in a 32x32 pixel subarray region of the detector. Two flat field (lamp on) and two background (lamp off) images are obtained. These F160W filter ACCUM images are taken immediately before the autonomous slew to move the image of the hole over the position of the target. Each set of images are combined by minimization similarly to the 128x128 pixel images, and then the processed background image is subtracted from the processed flat field image. The hole location/centration process must flat field the images of the soft-edged (afocal) coronagraphic hole, or pixel-to-pixel variations will bias the centroid solution. The “hole finding” FSW performs a flat field correction on the background subtracted flat field subarray image using a pre-loaded “gain table”. Unlike the 128x128 pixel gain table used to flat field the target images, the hole gain table is stored onboard as real (32 bit) numbers normalized to unity. The 128x128 pixel gain table is stored on board as integer (8 bit) numbers. Typical values range from 0.8 - 1.2.

The processed image is inverted by subtracting the image from a constant. A small 7x7 pixel checkbox is used to find the hole, and a 15x15 pixel checkbox is used to find the centroid of the inverted hole image. A weighted moment algorithm is applied to determine the flux-weighted centroid within the checkbox. The location of the hole is temporarily stored onboard, but it is not saved in the telemetry sent to the ground.

A list of targets and their characteristics, observed as part of the coronagraphic test programs, is presented in Table 1.

Table 1. Target characteristics.

program ID	target name	spc. type	V	H	H-K
8983	GSC 07183-01447	K7V	10.5	6.9	-
	GI 644C	M7V	16.7	9.19	-
8979	BD+032954	M0III	9.36	5.00	0.19
9693	BD+001694	K7	9.75	4.815	0.225

program ID	target name	spc. type	V	H	H-K
	BD+032954	M0III	9.36	5.0	0.190
	BD+323739	A4III	9.31	-	-

Operability of the TA FSW

A test program (ID: 8983) to determine the Mode-2 coronagraphic TA performance was executed during SM3B. It was thought that the performance of the onboard Mode-2 imaging processing might be degraded because the operating temperature is higher than that used during Cycle 7. The higher operating temperature has changed the characteristics of the detector; i.e, well depth, hot/cold pixels, bias, and dark levels. In addition, the performance might be compromised due to metrological changes caused by the dewar stress/relaxation resulting from the warm up and cool down of NICMOS.

To check and validate the onboard TA FSW, Mode-2 target acquisitions were performed on two “isolated” bright stars, GSC 07183-01477 and GL 644C. See Table 1 for target characteristics. Both of these targets were observed in Cycle 7. These SM3B observations confirmed that the Mode-2 acquisition software worked as expected. One calibration problem was found wherein the onboard flat field gain table used as part of the hole-location (CSPOT) algorithm had values which were incorrect by, typically, ~ 10-20%. This resulted in degraded determinations of the location of the fiducial point in the coronagraphic hole, and ultimately small (on the order of ~ 0.2 pixel) targeting “errors”. The cause of this is completely understood: a clerical error in the preparation of updated CSPOT gain table values that were uploaded to the NICMOS FSW’s patchable data area before the test. A new replacement table was delivered and uploaded to NICMOS (on July 28, 2003).

The location of the hole image on the detector has moved ~ (+2, +5) pixels in image space on the detector since January, 1998. The half-width of the afocal image to be processed by the hole centroid algorithm is 8 pixels, so the “edge” of the afocal hole image has moved to within 3 pixels of the currently defined 32x32 pixel subarray field-of-regard. Given the uncertain nature of the stability and “creep” of the hole location over time, it was decided to redefine the location of the hole field-of-regard as of June 1, 2002. The lower left corner (xmin, ymin) of the 32x32 pixel box is now at X=26, Y=164 (in FSW detector coordinates).

The two tests to probe the minimum flux limits required to achieve a successful acquisition (with a planned “underexposure” by a factor of ~10 in each case) failed. In HST Cycle 7 the system was tuned up so that a target exposed as shallowly as 5.6% of saturation could be located in the onboard hole location process. This is important for the acquisition of faint targets (such as for coronagraphic imaging of damped Lyman-alpha

systems, or companions for the coldest T dwarfs), where more deeply exposed TA images can take a significant portion of a target visibility period. These two targets, exposed to about the 7% level, were not found by the target-locate algorithm. This is fully understood as due to the change in the very end of the hot-pixel tail of the “dark current” distribution function. A few anomalous pixels have exposure-time dependent charge accumulations, which can appear as a signal brighter than a faintly exposed target. The FSW allows for “turning off” such pixels in the target locate/centroid algorithms by assigning a value of zero to these pixels in the gain table. A small handful of pixels in the target (not hole) gain table have been assigned a value of zero.

Analysis of dithered imaging data obtained following the nominally exposed target acquisition images in SMOV/8983 (Visits 03, 04, 13 and 14) indicate that a FSW (and PDB) update to the NICMOS Camera 2 aperture rotation angle was warranted. A correction of -10.76 ± 0.50 arcminutes (-0.1793 ± 0.0083 Deg) was made to the aperture rotation value yielding a new value of 224.75 ± 0.02 Deg (SIAF) as determined by Cox (2002). This corresponds to a differential rotation angle of $+3.84 \pm 1.32$ arcminutes with respect to the Cycle 7 rotation angle (uploaded on July 3, 2002).

A small systematic offset in the final target positions was found. These mispointings are on the order of ~ 0.3 -pixels and are most likely due to the aperture rotation angle not being up-to-date in the acquisition FSW. In addition, on June 10, 2002, the FSW was uploaded with a revised plate scale ($xscale=0.07588 \pm 0.0003$, $yscale=0.07537 \pm 0.0005$) (Cox 2002). These updates were determined from proposal 8982

Figure 1 presents comparative images showing a direct vs. coronagraphic vs. coronagraphic PSF-subtracted PSF from the SMOV/8983 test. The star used for the TA test was not as bright (about a factor of 10 less) than the one used for the Cycle 7 performance test and the exposure time did not go nearly as deep - as this was not a performance test. In the coronagraphic images, the systematic offset of the target from the fiducial point shows up as scattered light on the lower-left side of the hole, and results in much more scattered light at a low level. The improvement obtained over direct imaging is clear, but until the centering bias is removed, the performance is not as good as achieved in Cycle 7. The low scatter point offset has since been updated (on July 28, 2003).

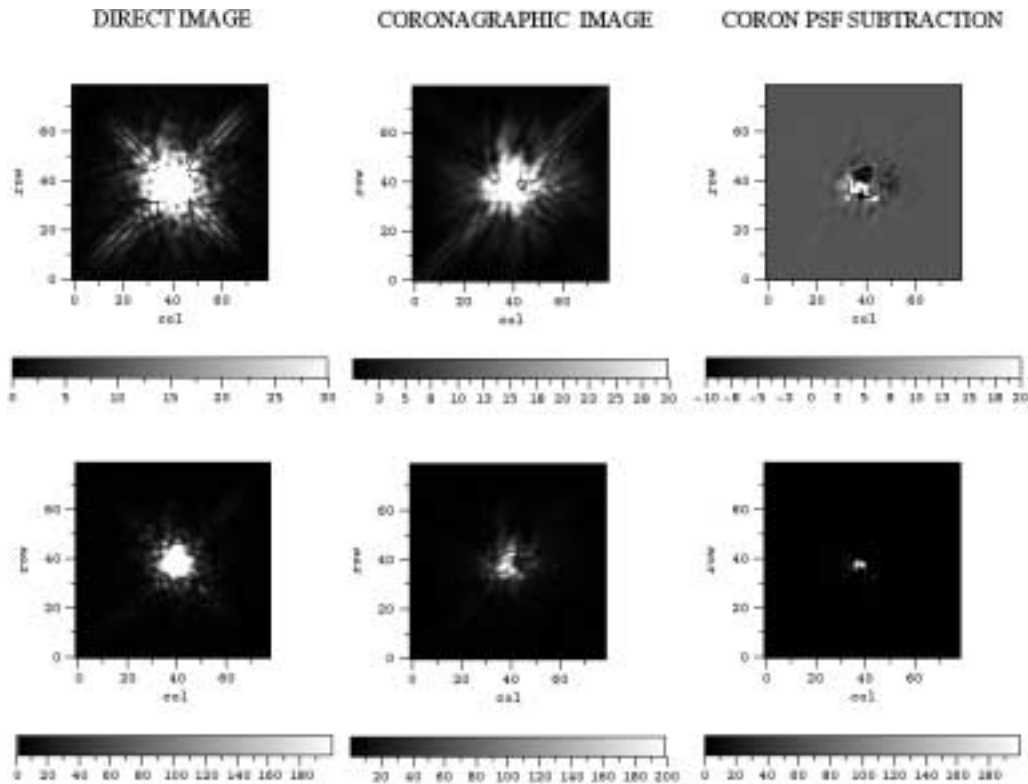


Figure 1: Comparative images showing a direct vs. coronagraphic vs. coronagraphic PSF-subtracted PSF from the SMOV/8983 test.

In addition, the first requested “POS TARG” following the ACQ was ignored. The database flag to indicate the necessity of a slew was not set because Transformation (TRANS) mistakenly assumed no pointing change would ever be needed when aperture NIC2-CORON follows aperture NIC2-ACQ. Subsequent POS TARGs were executed as planned. TRANS Operation Problem Report (OPR) 46041 addressed this issue and was closed in July 2002, so this problem should not occur again. The 8983 test was sufficiently robust that the loss of these data did not preclude meeting the primary test objectives.

Coronagraphic Focus (PAM position)

The NICMOS coronagraph was originally designed to have two foci at *conjugate* points in the optical path with the coronagraphic hole at the f/24 focus of the input Optical Telescope Assembly (OTA) beam, and the detector at the reimaged f/45 focus in Camera 2. Because of the forward displacement of the cold optical bench holding the Camera 2 detector, as a result of the larger-than-expected expansion of the solid N₂ cryogen, the two foci are now *a conjugate*. For direct imaging this is of little concern, and the HST/NICMOS Camera 2 focus interface is established by co-locating the f/45 image plane on the detector. This is done by de-spacing the relayed focus through a translative motion (with compensating coma tilt correction) of the Pupil Alignment Mechanism (PAM). The mir-

ror, driven by this mechanism, is upstream of the field-divider mirror upon which the coronagraphic hole resides. Therefore, achieving a “best” focus at the detector results in a “soft” focus (in the f/24 image plane) at the coronagraphic hole. This leads to a wavelength-dependent increase in the diffracted energy in the now defocused unocculted wings of a PSF from a target placed inside of the coronagraphic hole (as the f/24 image plane will fall behind the surface of the Camera 2 field divider mirror) increasing the scattered and diffracted background around the target and lowering the field contrast at the detector image plane. In principal the coronagraphic stray light rejection would be most efficient by minimizing the spot size of an input PSF in the hole. This, however, is traded against a small degree of defocus at the detector. Ultimately, the best coronagraphic performance is achieved where the image contrast between an unocculted target and the residual background from an occulted source (both affected differently by focus and subsequent scattering) is maximized. Further details and background information may be found in the SMOV/7157 test report “NICMOS Optimal Coronagraphic Focus Determination¹”.

The test program (ID: 8979) was executed to find the optimum PAM position to maximize the coronagraphic image to background contrast ratio. A series of coronagraphic images was obtained at various PAM settings; i.e., (A) in-focus image formed at the detector, the nominal Camera 2 (PAM2) focus position for direct imaging, (B) at a point where the image planes formed at the field divider assembly (FDA) and detector evenly split the focus error, and (C) with the image in focus at the FDA (current PAMC position). The target for this test was BD+032964. See Table 1 for target characteristics.

No focus adjustment was necessary for the Camera 2 coronagraphic focus (PAMC). The nominal Cycle 7 PAMC focus position was the correct setting. This result was not unexpected as the coronagraphic focus position is at the f/24 focus of the input OTA beam, which is outside the dewar.

Coronagraphic Performance (PAM tilt)

The Mode-2 target acquisition process requests a spacecraft slew to position a target into the coronagraphic system after locating both the coronagraphic hole (which is unstable at the sub-pixel level with multi-orbit time scales) and the target. The FSW’s photocentric determination of the position of the hole is not the point at which an occulted target will have its total diffracted+scattered energy minimized by established criteria. The “low scatter point” (referred to by some as the “sweet spot”) is offset from the hole photocenter by a small amount. This offset, in X and Y, is stored in the flight software and added to the slew request so the target will fall onto the low scatter point. The low scatter point offsets are held in the NICMOS FSW as “tunable constants” and were set to non-zero values as a result of the SMOV Cycle 7 coronagraphic commissioning program. These values are

1. available from the NICMOS IDT, URL <http://nicmosis.as.arizona.edu:8000/Publications.html>

expressed in units of 1/50 pixel and are in the FSW detector coordinate system, not in SIAF coordinates.

A test program (ID: 9693) to determine the coronagraphic performance was executed during Cycle 11 and 12. Three different targets were observed: BD+001694, BD+032954, and BD+323739. See Table 1 for target characteristics. Analysis of these test data indicated that a significant improvement in coronagraphic background light rejection in the close environment of the coronagraphic hole can be achieved by positioning a target +0.2 pixels along the image Y axis (SIAF) from the current Mode-2 position. An offset of -0.2 pixels in X was added to the FSW tunable constant offset to reposition targets at the new low scatter point. During Cycle 7 and 7N, the low scatter point was at pixel location $x=-0.75$, $y=-0.25$ (SIAF) from the hole center. It is now at $x=-0.75$, $y=-0.05$ (SIAF) pixels from the center of the hole (uploaded July 28, 2003).

Following the upload of the tunable constants in the FSW, the Mode-2 slew following the onboard hole and target location centroids successfully positioned the target to the desired coronagraphic hole low-scatter point. This was performed twice due to the somewhat different slew vectors caused by rolling the telescope between two visits in the same orbit. The target was in different positions in the two acquisition images as were the guide stars in the FGS field-of-view (pickle positions). In both cases, the target was acquired within approximately 0.08 pixel (~ 5.8 mas) of the absolute low-scatter position, with a repeatability of 0.04 pixel (~ 2.9 mas), which meets the requirement given the error budget for onboard processing of the images.

The “out of hole” images which executed in 8983 and 9693 showed degraded coma image quality for non-occulted targets in the field. The images were taken with the PAMC X,Y tilts set to those used for Cycle 7. This small amount of coma was not present during Cycle 7 and does not affect the current determination of the low scatter point offsets. The same differential changes in X,Y tilt from nominal applied to PAM2 tilt positions were applied to the PAMC tilt positions. This small tilt adjustment was sufficient to balance the flux in the star images. The Cycle 12 Camera 2 PAM focus positions and tilt values are given in Table 2 (uploaded November 3, 2003).

Table 2. Cycle 12 Camera 2 nominal focus positions in mm of PAM motion and tilt positions.

	PAM2	PAMC ^a
Focus	0.20	2.69
X,Y tilt	15,10	15,14

a. PAMC is the best focus position for Camera 2 coronagraphy.

The NICMOS coronagraphic observing mode has been fully recalibrated. Figure 2 presents coronagraphic imaging of the same target obtained during Cycle 7 and 11 showing the repeatability of the observing mode over many epochs. Observations of the target were obtained in a single orbit with a roll of the telescope between visits. This allows self-subtraction of the underlying coronagraphic point-spread function. Note that the top-left to bottom-right diffraction spike residuals have vanished (or nearly so) in image B (Cycle 11) compared to image A (Cycle 7). This is due to better alignment of the pupil mask central support. However and unfortunately, the other diffraction spike has gotten worse. The faint companion is at ($\rho=2.5$ arcsec) and clearly indicates that detection of faint companions in close ($\rho < 1$ arcsec) to bright stars is achievable with NICMOS.

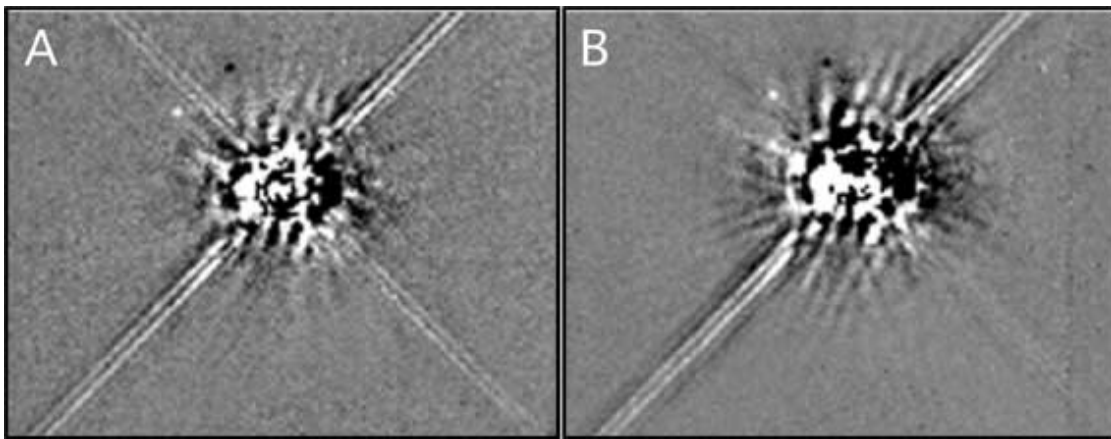


Figure 2: Cycle 7 (A) and Cycle 11 (B) coronagraphic observations of TWA6 (F160W) obtained in the same orbit with a roll between observations. A faint candidate companion ($H=20.1$, $\Delta H=13.2$, $\rho=2.5$ arcsec) is to the upper left of the PSF subtraction residuals (3σ detection). The candidate companion was rejected due to non-common proper motions. Note the “smooth” background in image B (Cycle 11) compared to A (Cycle 7). This is due to the improvement in QE following the installation of the NCS (Schneider 2002).

Conclusions

The NICMOS coronagraphic imaging mode has been fully reactivated following SM3B, and it performs slightly better than during Cycle 7. The diffractive rejection is essentially unchanged (to first order) from Cycle 7 except there is a shift in the mean position of the cold mask which gives better second-order rejection on the downsloping diffraction spikes and slightly worse on the upsloping diffraction spikes. The effect on the PSF core is minimal. If the position angle (PA) of a target is *a priori* known, one can use this to advantage by constraining the roll of the observation.

The Mode-2 acquisition FSW performed as expected. The target location/centroid performance is identical to Cycle 7, as per spec. Some adjustments to the coronagraphic system parameters were necessary. The hole 32x32 pixel field-of-regard was adjusted

slightly due to displacement of the hole image on the detector caused by the warm up at the end of Cycle 7 and subsequent cool down following SM3B. The location of the hole image on the detector was found to be more stable than in Cycle 7. A new “gain” table (flat field) was installed to handle hot and cold pixels, allowing Mode-2 acquisitions for targets from H=4 to 17. A slight adjustment was made to the Camera 2 aperture rotation angle, a correction of -10.76 ± 0.50 arcminutes (-0.1793 ± 0.0083 Deg). The coronagraphic focus was checked and no adjustment was needed. The coronagraphic hole low scatter point, the “sweet spot”, was checked and a slight adjustment of $+0.2$ pixels along the image Y axis (SIAF) was performed. A slight adjustment was made to the PAMC tilt to remove some coma that was not present during Cycle 7. This yields slightly better image quality for non-occulted targets in the field than in Cycle 7.

An overview of NICMOS coronagraphy from its inception on February 8, 1998 through December 18, 1998 is presented in Fraquelli et al. (2004). During this time interval, which corresponds to HST Cycles 7 and 7N, coronagraphic observations of 329 targets for 22 programs were obtained.

Recommendations

NICMOS coronagraphy is extremely sensitive to small centering errors caused by changes in the plate scale and to hot pixels. It is recommended that at least once a year a determination of the NIC2 plate scale be performed and if necessary, the Mode-2 FSW plate scale be updated. In addition, hot pixels should be monitored for any changes that might affect the acquisition of faint targets and the corresponding pixels in the gain table updated.

The NICMOS coronagraphic imaging capability is a unique HST resource. During Cycle 7 and 7N, it was used to search for and/or confirm the presence of planetary and brown dwarf companions around nearby stars, to probe the structure of circumstellar disks, and to study the host environment of quasars with damped Lyman alpha systems. These programs, and others, are expected to continue during future observing cycles. To enhance the scientific return from coronagraphy, coronagraphic observers are advised to request flat field observations (lamp-off and lamp-on observations) to capture the instantaneous position of the coronagraphic hole at the time of the science observations. This request must be fully justified in the Phase I proposal.

Acknowledgements

We would like to thank the STScI Flight Systems Engineering (FSE) group for tracking down critical information about the NICMOS FSW, the all important dates that changes were uploaded, and for installing the ACQ FOR gain table twice within on year. We also want to thank OPUS for their quick turn around on fast tracking the coronagraphic calibration data and for their patience while tracking in real time the success or failure of coronagraphic ACQs.

References

Cox, C. 2002, private communication.

Fraquelli, D., Schultz, A.B., Bushouse, H., Hart, H.M., and Vener, P. 2004, *PASP*, 116, 55.

Schneider, G. 2002, "Coronagraphy with NICMOS," in 2002 HST Calibration Workshop, ed. S. Arribas, A. Koekemoer, Brad Whitmore, STScI, 249.

Schultz, A.B., Noll, K., Storrs, A., Baggett, W., Sparks, B., and Fraquelli, D. 1998, "NICMOS Coronagraphic Acquisition", NICMOS Instrument Science Report, NICMOS-97-031.

Schultz, A.B., Noll, K., Storrs, A., Bacinski, J., Baggett, W., and Fraquelli, D. 1998, "NICMOS Camera 2 Coronagraphic ACQs," NICMOS Instrument Science Report, NICMOS-98-012.

Appendix I - Pick an ACQ Filter

NICMOS target acquisition (TA) integration times are generally short and should be designed to avoid saturation, but must produce enough flux to obtain a well-determined image centroid. Seventy-percent of full-well is the "target" exposure depth recommended by the NICMOS IDT. At the "bright limit" (for stars with $H < 4.0$ under the F187N filter) integration times must be chosen to allow centroiding using the wings of the PSF.

The TA images are flat-fielded via a single onboard calibration table, the "gain table". This table holds the pixel-to-pixel responsivity multipliers appropriate for the detector response in H band (F160W). The gain table also works well for F165M and F170M filter ACQ images, and within the target acquisition error budget even out to the F190N filter. Shorter wavelength (F110W) and longer wavelength filters are improperly flat fielded, and yield incorrect weights to the pixels which are used in both the target locate and image centroid solutions. At even longer wavelengths, issues of thermal background can become an issue for acquiring faint targets. The coronagraphic hole is thermally emissive at long wavelengths and presents a high background of its own near the hole edge.

In addition, Camera 2 undersamples the PSF at F110W. The half-width to half-maximum intensity of the PSF core is at a distance of only 0.8 pixels from a well centered PSF's photocenter, and the first Airy minimum occurs at 2.0 pixels. Hence, even following a successful target location (which "finds" the target to the nearest pixel), the spatial content of the F110W PSF is insufficient in this undersampled domain to obtain a high precision centroid solution using the photocentric weighted moment algorithm implemented by the FSW to correctly place the target in the coronagraphic hole. The FSW

algorithm works best when the PSF is at least approximately critically sampled. This precludes filters short of F160W for ACQs, which for Camera 2 is the F110W filter.